LA-UR-91-2703

LA-UR--91-2703

DE91 018037

Los Alamos National Laboratory is operated by the University of California for the United States Department of Energy under contract W-7405-ENG-36

TITLE EXPERIMENTAL EVALUATION OF A CONTACT AREA EVOLUTION MODEL

AUTHOR(S) David Korzekwa, MST-6
P. R. Dawson, Cornell University

SUBMITTED TO ASME Symposium on "Tribological Aspects in Manufacturing"
at the 1991 Winter Annual Meeting
December 1-6, 1991
Atlanta, GA

DISCLAIMER

Los Alamos National Laboratory
Los Alamos, New Mexico 87545

Experimental Evaluation of a Contact Area Evolution Model

D.A Korzekwa
Los Alamos National Laboratory

P.R. Dawson
Cornell University

Abstract

Experiments designed to simulate boundary lubrication conditions during sheet forming were performed and evaluated. The results are compared to a model for contact area evolution caused by flattening of surface asperities. Microscopic observations and estimates of the area fraction in boundary contact agree reasonably well with the model. The effect of microstructural features on the accuracy of continuum models is also discussed.

Introduction

The development of physically based models for friction during metal forming is important for a better understanding of friction and to enhance simulation capability. Models have been proposed based on state variable methods that use the surface roughness, lubricant properties and flow strength of the workpiece as variables[1,2,3,4]. Verification of these models is necessary to evaluate their accuracy and range of applicable conditions. Experiments to identify mechanisms and measure the relevant parameters at the interface are usually difficult, and it is important to duplicate the conditions that are present in the forming operation.

One important variable is the fraction of the apparent area that is actually in boundary contact at a given time during forming. The contact area can change considerably during a metal forming operation and will typically vary at different locations on the tool-workpiece interface. This change is due to the change in lubricant film thickness during the operation and the flattening of surface asperities. This article will describe work to model and verify these changes for conditions relevant to sheet forming.

Description of the Model

It has been observed that the actual contact area during metal forming is often much greater than that for the surfaces of two non-deforming objects in contact[5,6,7]. Models have been proposed to explain this effect based on the asperity flattening mechanism illustrated in Figure 1. It is assumed that for small asperity angles θ the deformation is similar to indentation of a flat surface by a flat punch. The problem is posed in terms of the dimensionless quantities E, A, H and φ defined as follows:

$$E = \frac{d_{ll}}{v_l}, \tag{1}$$

$$A = \frac{a}{l}$$

$$H = \frac{P_a}{k} \tag{3}$$

$$\phi = \tan^{-1}\left(\frac{\bar{d}_{yy}}{\bar{d}_{xx}}\right). \tag{4}$$

The variables are defined in Figure 1 except for k, the flow strength in shear of the material and d_{ij}, the components of the deformation rate tensor in the bulk material. The strain direction parameter φ is defined for the case where the asperities are two-dimensional with the long axis of the asperities in the y direction. The x direction is transverse to the asperity lay (the horizontal direction in Figure 1). One further restriction in the model is that the principal strain directions must be aligned with the axes of the asperities.

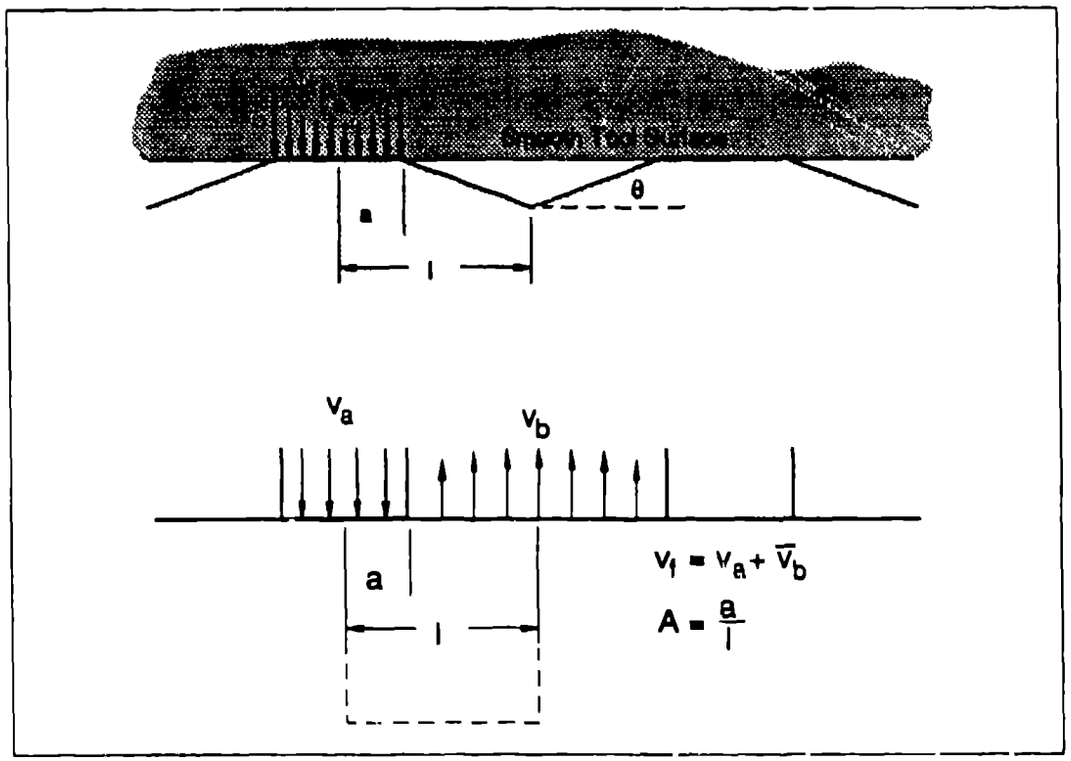

Figure 1. Asperity deformation model with trapezoidal asperities or flat indenters.

This problem was analyzed with a viscoplastic finite element program to determine the relationship between E, A, H and φ[5]. Using the meshes for shown in Figure 2 the velocity boundary conditions were varied to give different values of E, A and φ. The normal load on the top surface is calculated to give H. The results can be used to determine an instantaneous flattening velocity for a prescribed bulk deformation rate and pressure on an asperity.

The results imply that asperities will flatten at relatively low pressures when the underlying bulk material is deforming plastically. A physically based model for friction at the interface should include the contact area fraction A as a state variable, and the model described here should provide an evolution equation for A for some situations.

The results of the model were used to predict the growth in contact area fraction A for the regular asperity array in Figure 1 by integrating[1]

$$\frac{dA}{dt} = \frac{\sigma_n}{E\theta}. \qquad (6)$$

The conditions for the plots in Figure 3 were chosen to be appropriate for sheet forming. For the case of sheet metal forming the lubrication conditions generally involve boundary contact, and large contact area fractions have been observed[7,8]. The model predicts that the contact area increases rapidly initially and continues to increase significantly at relatively large strains.

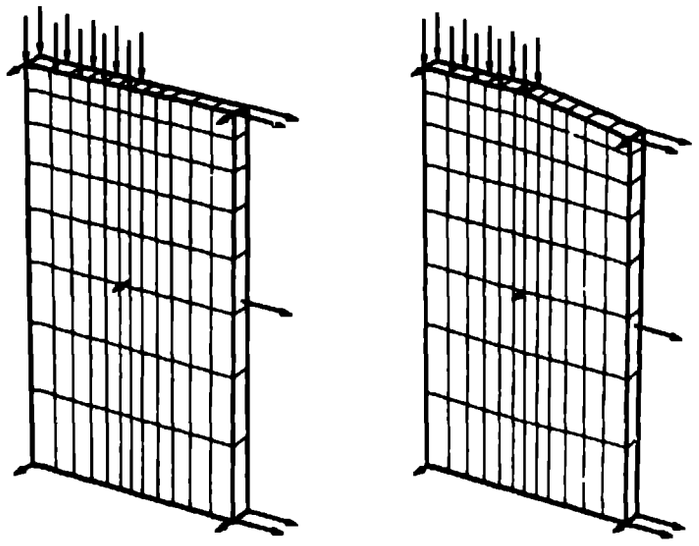

Figure 2. Mesh and velocity boundary conditions for ISAIAH simulations with $A = 0.5$.

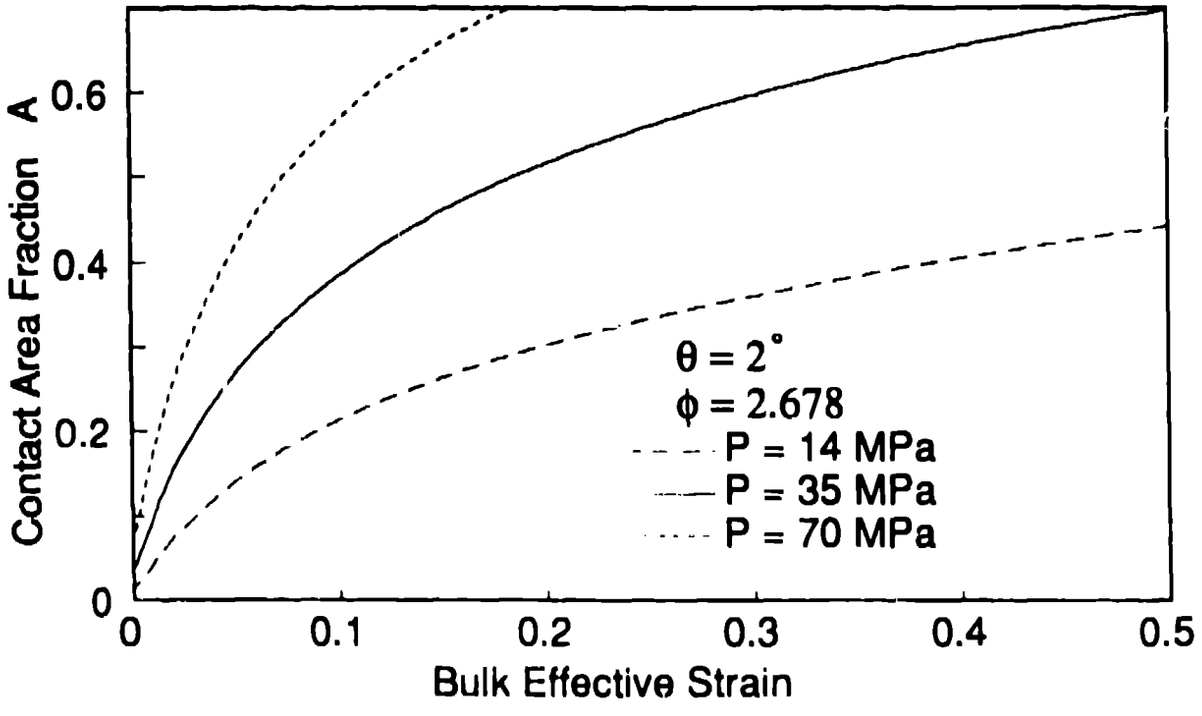

Figure 3. Contact area evolution with strain as predicted by the model.

In order to try to experimentally verify the contact area growth as predicted by the model, an in-plane drawing fixture was built to produce small sheet specimens with controlled strain and normal pressure histories. The specimen, die, and plate that acts as the tool surface are illustrated in Figure 4. As the specimen is pulled through the die the strain path is similar to that for the flange area in a circular deep drawing operation.

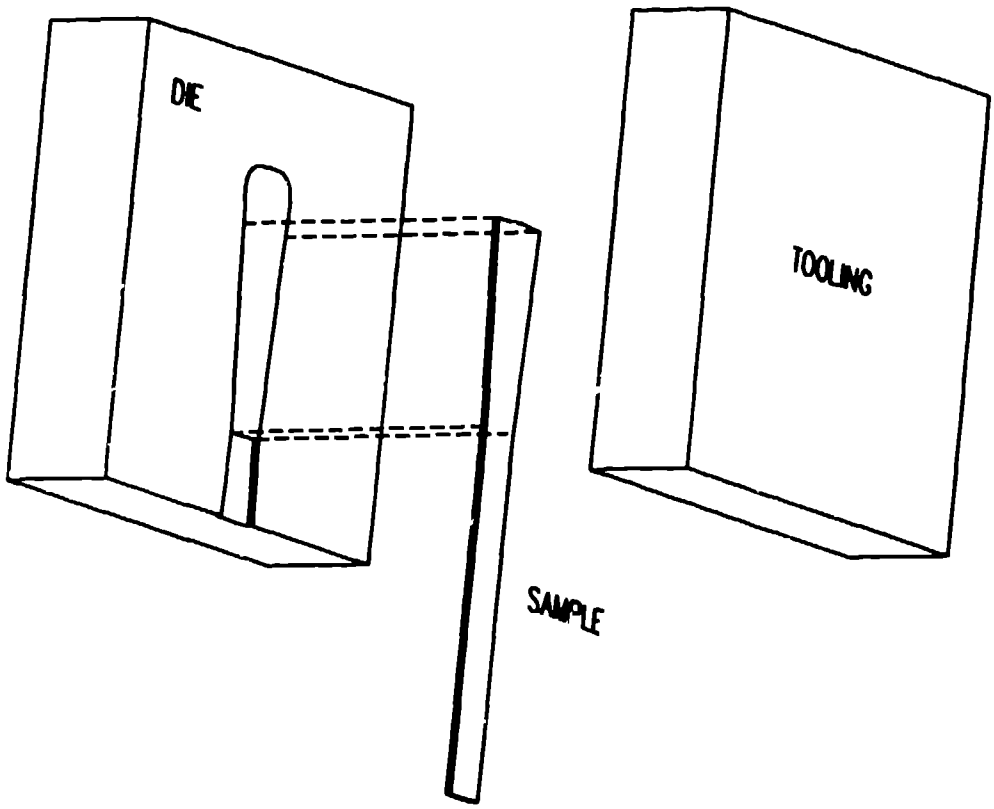

Figure 4. In-plane drawing sample with the die and tool surface plate.

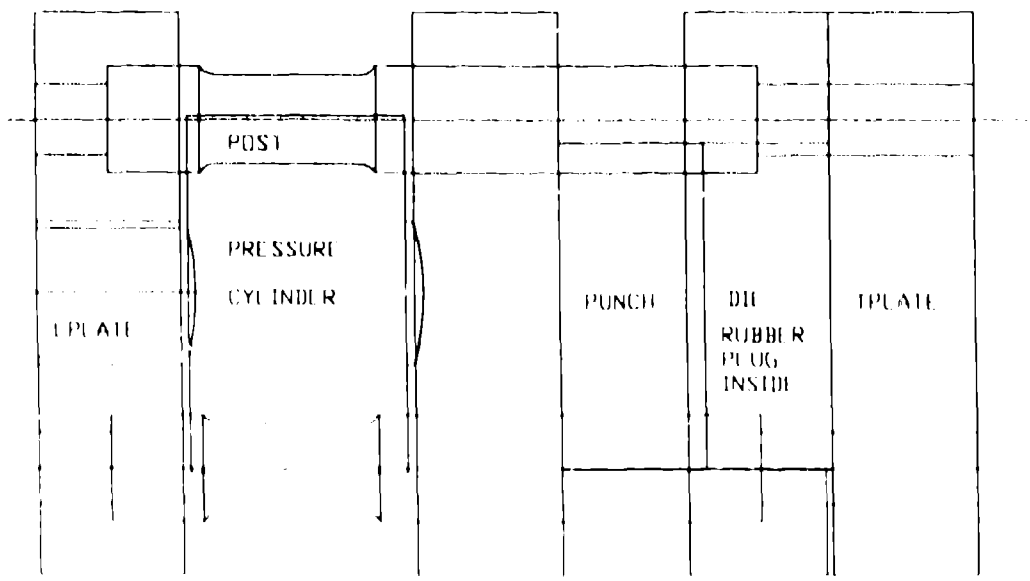

Figure 5. In-plane drawing fixture.

that fits in the die. A sketch of the mechanical components of the system is shown in Figure 5. The posts have strain gages that allow accurate measurement of the normal force applied by the punch by means of the hydraulic cylinder. The fixture is attached to a hydraulic load frame and the specimen is pulled out of the die at a constant velocity. The tensile load on the specimen and the load on each of the four posts are recorded digitally. A circle grid is electroplated on the side of the specimen that is not in contact with the tool plate, and the strain components in the sheet are measured at the end of the test.

The surface profile of the specimen is measured transverse to the roughness lay before and after testing at various points along the length of the specimen. A mechanical stylus profilometer is used to record the unfiltered profile signal at 0.5 micron intervals with a 12 bit A/D converter and a personal computer. The total effective strain and principal strain components are measured from the circle grid. The surface of the specimen is also examined with a scanning electron microscope (SEM) to qualitatively characterize the roughness changes.

Experimental Results

The preliminary results presented in this article are for a commercially produced 304L stainless steel sheet 0.66mm thick. The sheet was chosen because it has a surface profile that is generally consistent with the two-dimensional asperity assumption in the flattening model. Figure 6 is an SEM micrograph showing the condition of the surface as received. The asperities are very long in one dimension, which is also illustrated in the longitudinal and transverse profiles in Figure 7.

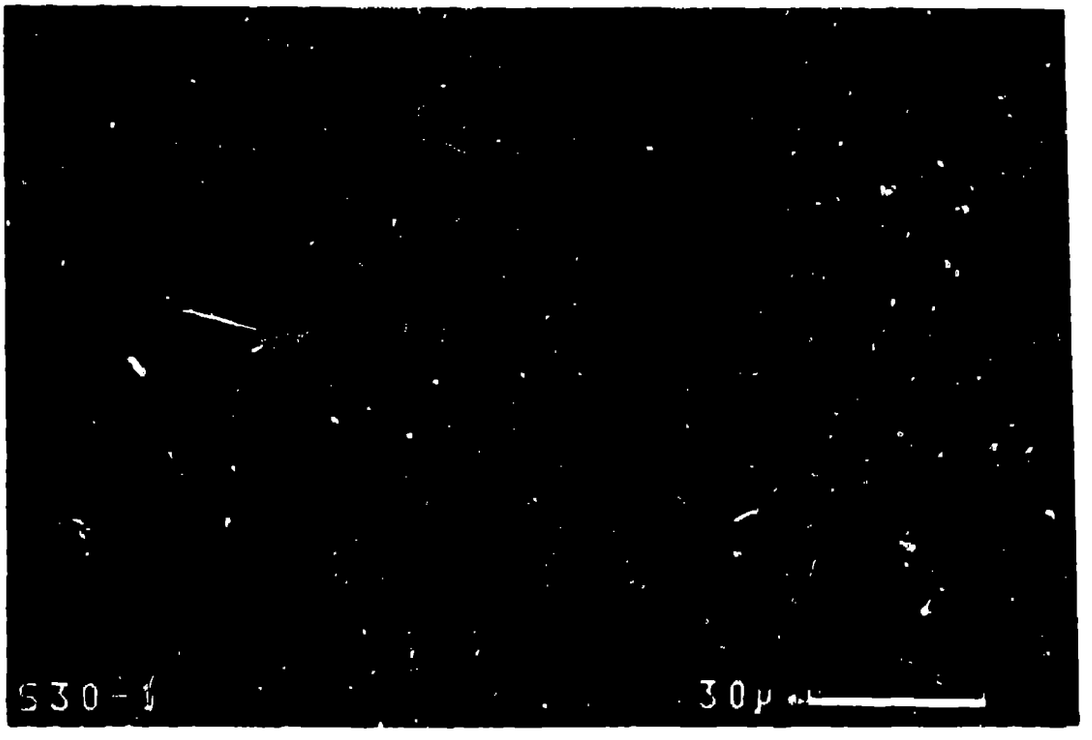

Figure 6. Scanning electron micrograph of the 304L surface before testing.

A sample of this sheet with the roughness lay oriented transverse to the axis of the sample was tested with an average normal pressure of 46.7 MPa, resulting in the strain distribution shown in Figure 8. The direction of sliding was transverse to the long axis of the asperities. The sample was treated with a commercial lubricant to form a boundary film, but there was no measureable liquid on the sample prior to testing. An SEM micrograph of a selected area of this sample shows flattened areas that qualitatively match the behavior predicted by the model (Figure 9). The area in Figure 9 is typical of most of the sample, and exceptions will be discussed later.

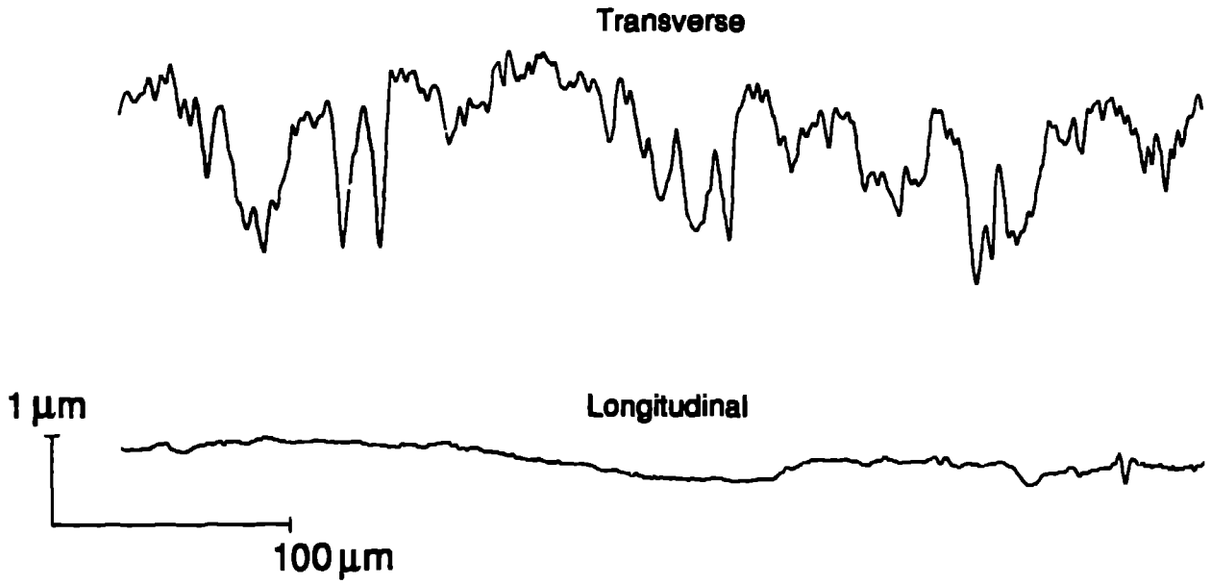

Figure 7 Measured surface roughness profiles for the 304L stainless steel sheet.

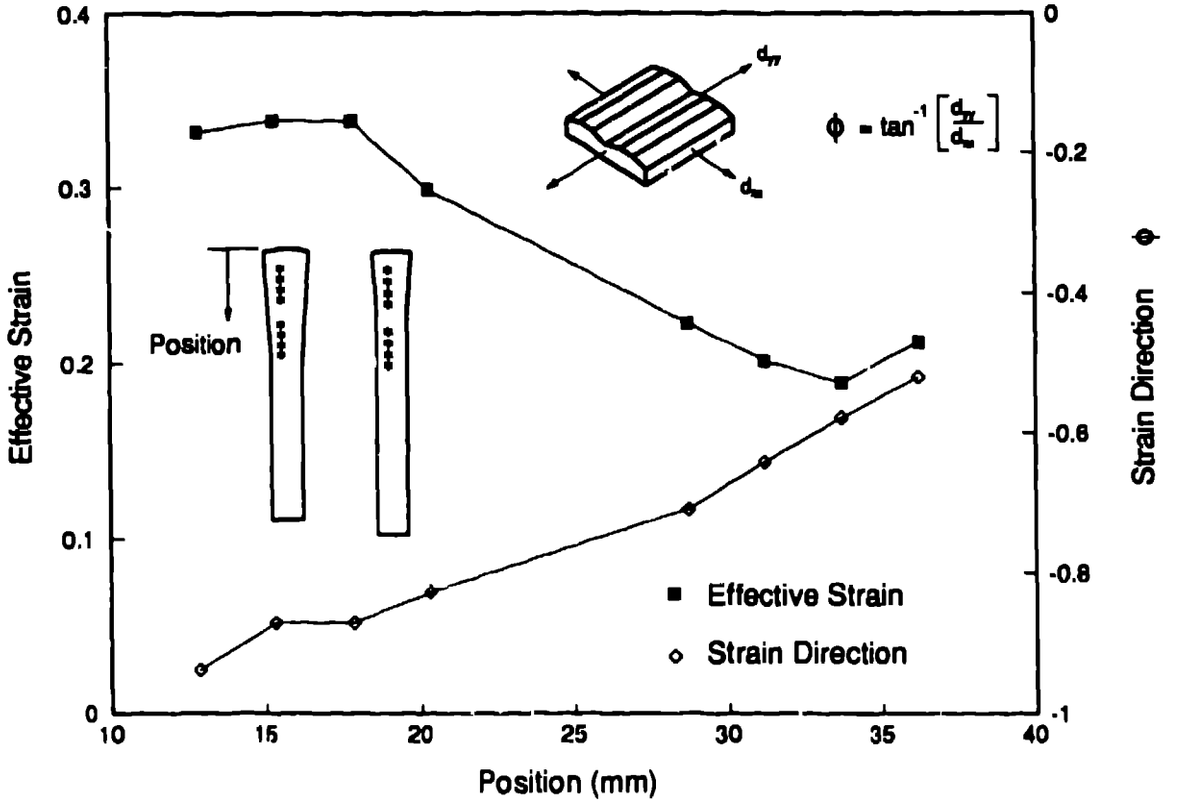

Figure 8. Strain magnitude and direction for the in-plane drawing test specimen.

Another way to look at the changes to the surface is to compare the frequency distributions of the height before and after testing (Figure 10). Note that the negative tail of the distribution is not substantially changed, indicating that much of the material between contacting asperities moves upward uniformly as the peaks are flattened. This agrees well with the assumptions of the model[4].

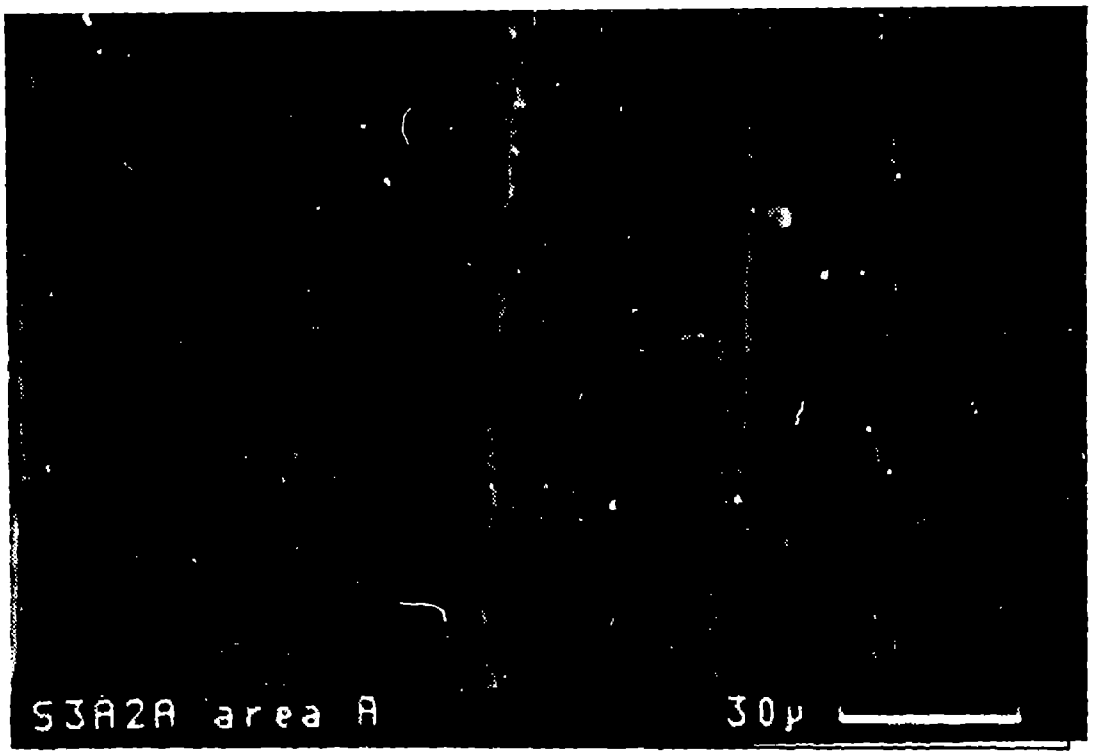

Figure 9. The 304L surface after testing.

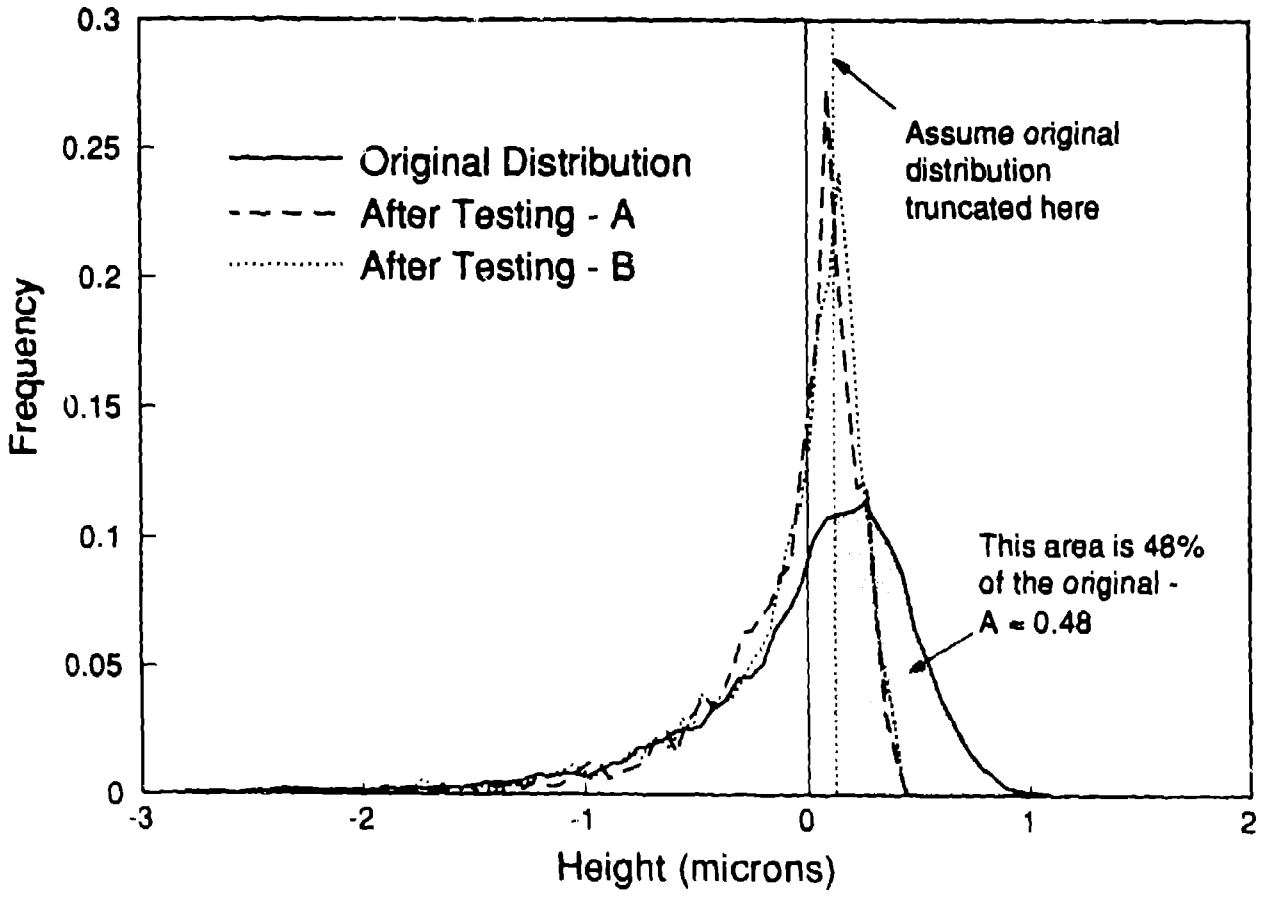

Figure 10. Height distributions before and after testing at one point on the specimen.

ideal flat tool and there was no elastic springback, the initial height distribution would be truncated with a sharp delta function at the height of the flat contacting areas. It seems reasonable to take the height value for the peak in the distribution measured after testing and truncate the original distribution to get a value for the contact area fraction. Results will be presented later based on this type of estimate as illustrated in Figure 10.

Some of the measured distributions show a narrow, well defined peak as in Figure 10, while others are more difficult to interpret. In many of the ambiguous cases the SEM shows significant roughening of the surface caused by inhomogeneous deformation of individual grains at the surface of the sample (Figure 11). This microstructural effect illustrates the type of problems that arise from applying a continuum model to length scales where microstructural effects are important.

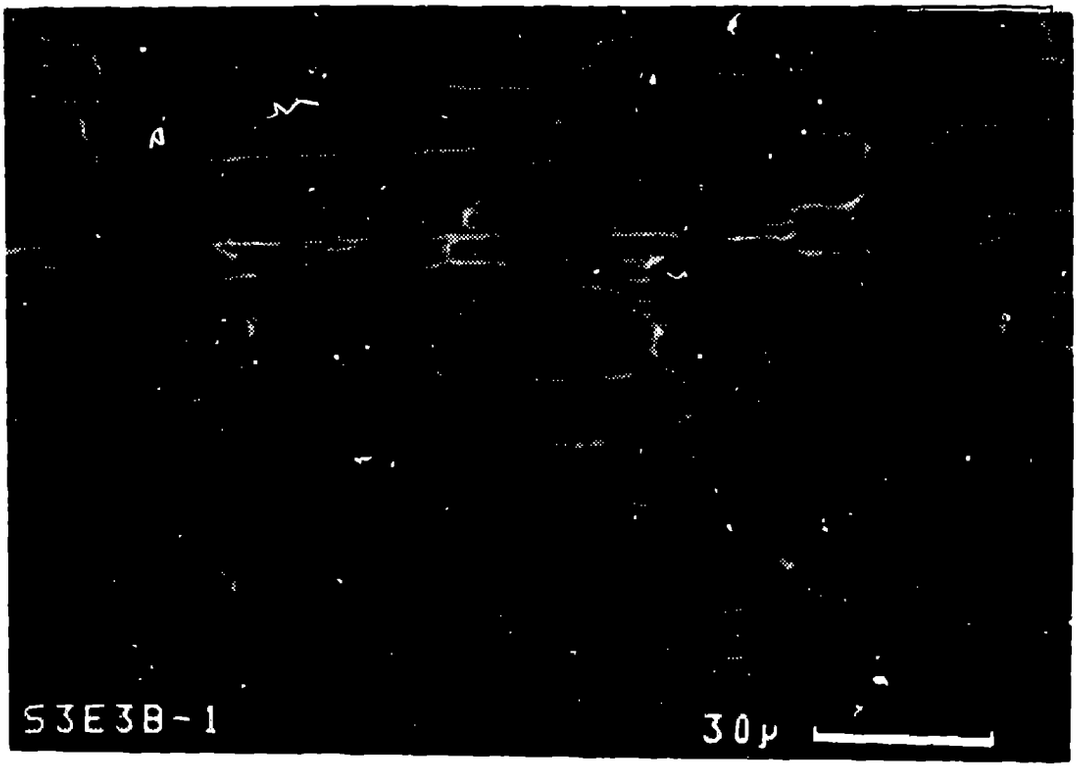

Figure 11. A region of the surface showing grain size roughening.

Another such effect is illustrated in Figure 12 where the homogeneity of the surface is considered. It is useful to estimate the minimum sample of the surface that is statistically similar to a large sample that represents the whole surface. This minimum distance defines the spatial resolution of the state variable model. Profiles transverse to the roughness lay were measured on five different specimens of the 304L stainless steel. The five profiles were combined after filtering and subtracting the mean line and used as a large (N=95000) sample representative of the surface as a whole. The five original samples were analyzed individually and broken into lengths of 5 mm, 2 mm and 1 mm. The shorter samples were each analyzed individually. The mean and standard deviations of the arithmetic average and root mean square roughness values were plotted as a function of sample length.

The mean values of the roughness amplitudes for the various profiles do not deviate significantly from that of the large sample, but the standard deviation increases sharply as the sample length decreases to less than 5 mm. This indicates that the surface profile is not homogeneous on a scale of less than 5 mm.

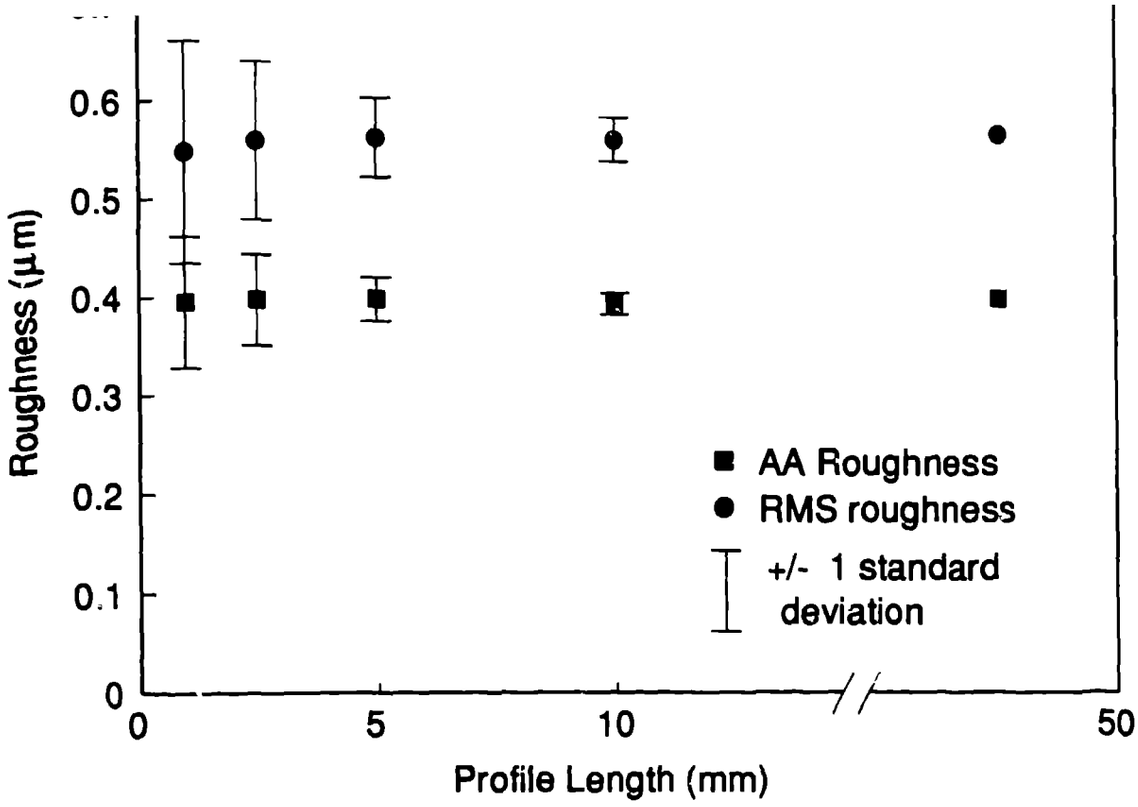

Figure 12. The mean and standard deviation of the roughness amplitude of 304L #4 as a function of profile sample length.

Comparison with the Model

The initial roughness profiles were used in conjunction with the relationship derived between E, A, H and φ to predict the contact area fraction for the stainless steel test sample. Two methods were used to extract the asperity geometry from the roughness profiles. In both cases it is assumed that as the asperities on the surface are flattened the material between the asperities moves upward uniformly over the region that is considered a material point. This assumption defines the kinematics at the surface and is equivalent to truncating the profile at the value of z corresponding to the plane of the tool surface as shown in Figure 13.

The approach used here for calculating the evolution of A requires that the flattening velocity v_f or dz/dt be calculated for given values of A, P, d_{II} and φ. The value of A is related to a value of z that corresponds to a collection of asperities in contact with the tool. Two methods were be used to convert the distribution of contacting asperities to the dimensionless variables in the flattening model. The simplest approach is to find the average contact area A and the average contact spacing l, and evaluate E and v_f as if it were for an array of uniform asperities. The other approach chosen is to impose a constant velocity on each asperity individually, sum the resulting pressures, and iterate to find the velocity that produces the actual applied pressure at the interface.

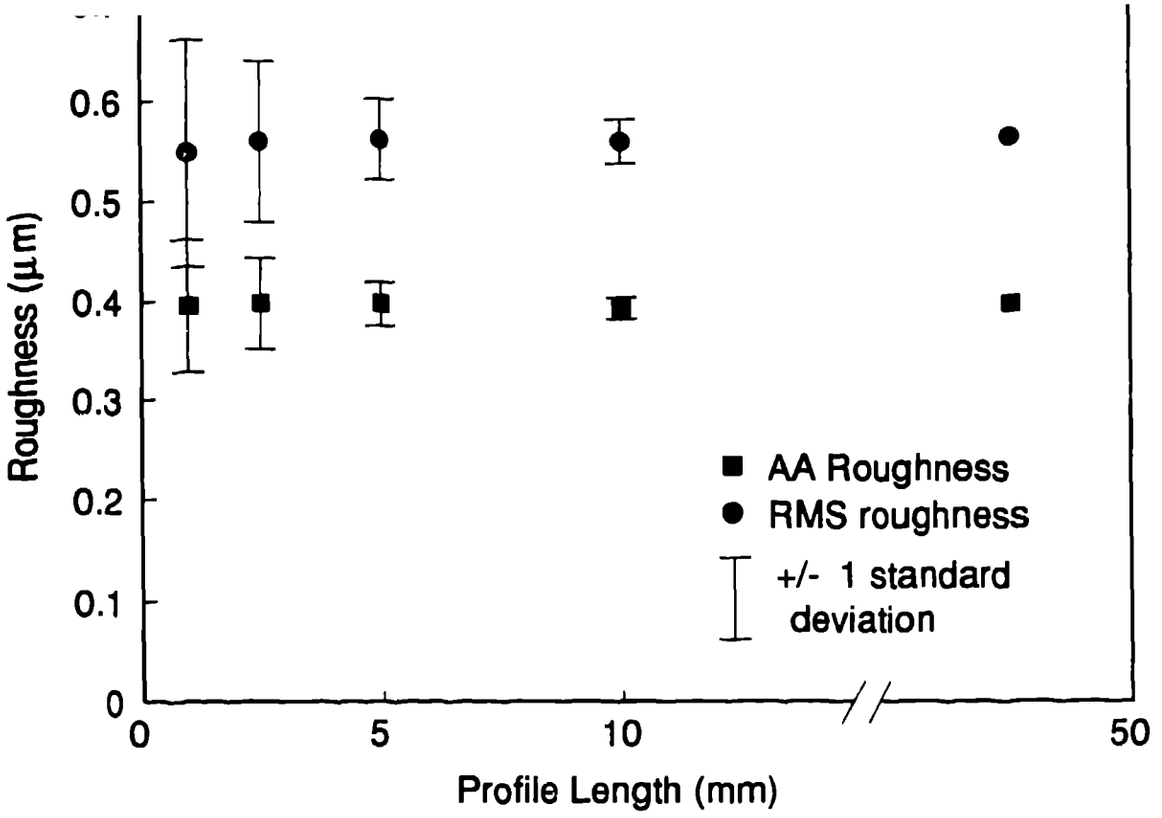

Figure 13. The mean and standard deviation of the roughness amplitude of 304L #4 as a function of profile sample length.

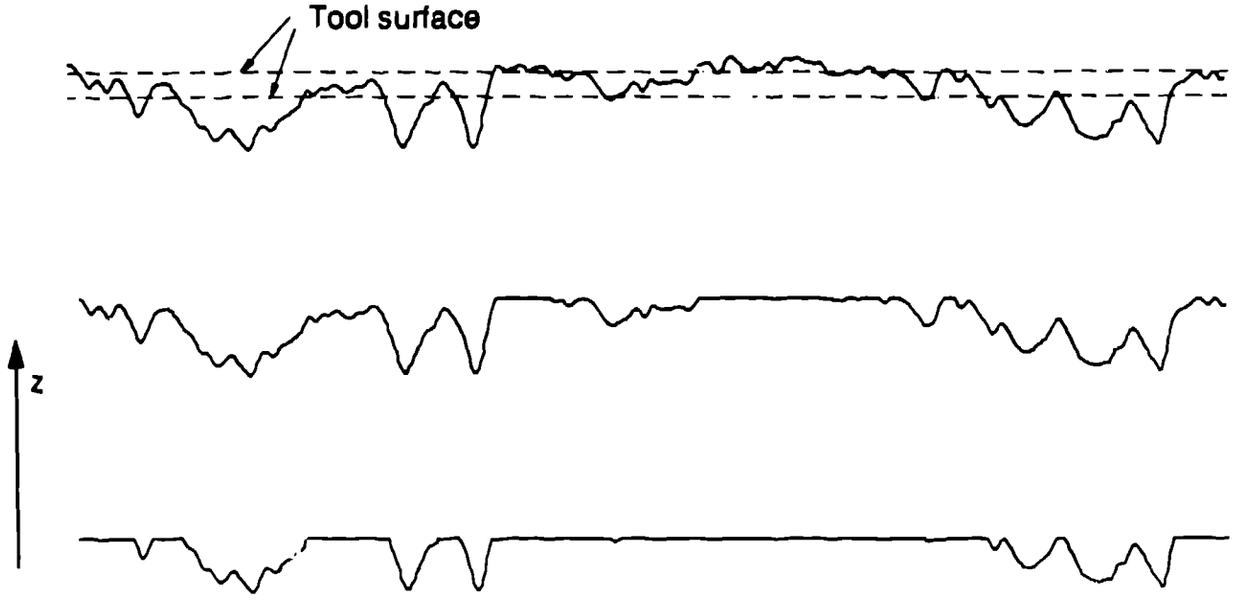

Figure 14. Flattening of asperities by truncating the profile.

The contact areas predicted by the model and estimated from the measured height distributions are shown in Figure 14 for the 304L sample with the final strain distribution shown in Figure 8. Each data point is estimated from a 2.5 mm profile. Note that these profiles are shorter than the minimum length necessary for the con-

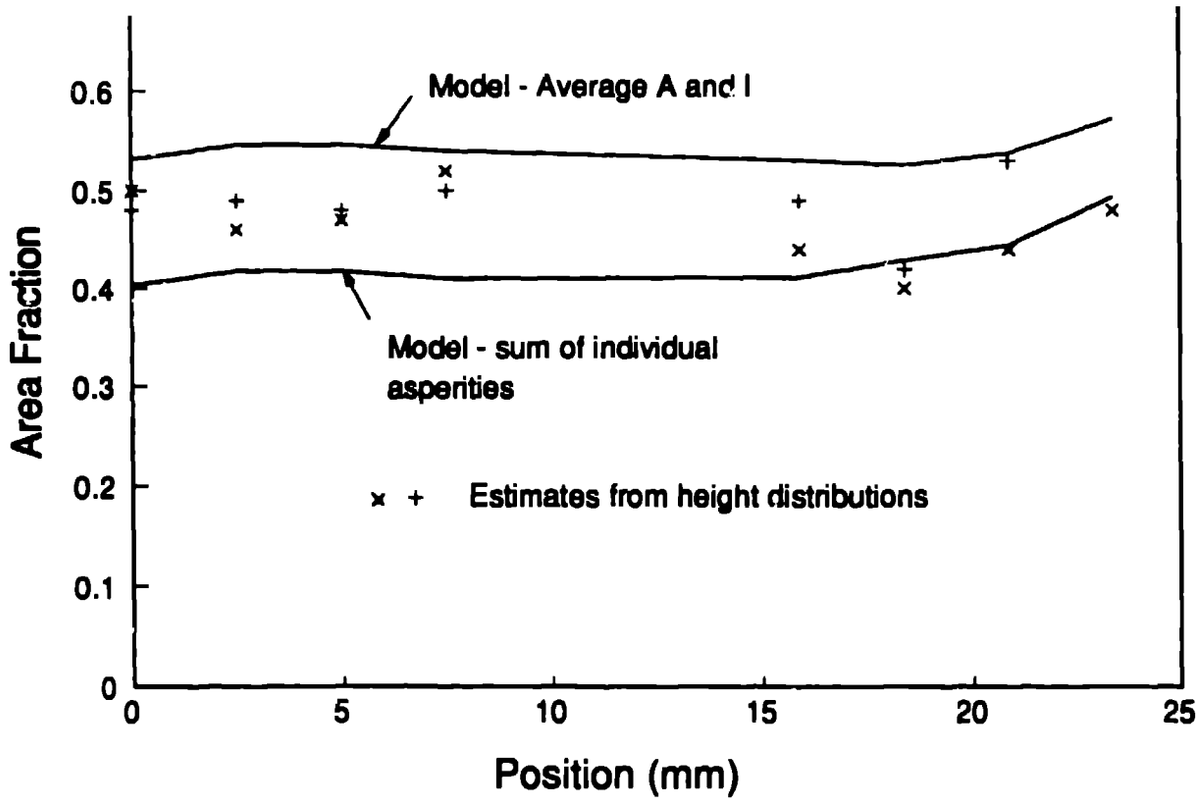

Figure 15. Comparison of measured contact areas with the model.

tinuum point assumption. The agreement between the experimental estimates and the model predictions is reasonably good, with most of the data lying between the two predicted curves.

Conclusions

The limited experimental evidence presented here generally supports the use of the asperity flattening model for calculating the contact area fraction during sheet forming. The microstructural examination and statistical profile analyses are consistent with large increases in the actual contact area, and there is quantitative agreement between the estimated area fraction and the model calculations to within about 10%.

It must be noted however, that this boundary contact model does not include any lubricant effects. If a liquid lubricant is present it is necessary to couple this model with a fluid flow calculation to determine the fraction of the normal pressure that is supported by the lubricant. This model also does not address the mechanisms that produce the friction traction at the areas in boundary contact.

A note of caution is also in order concerning the application of continuum models for friction. The microstructures of the interface and the bulk material are often not homogeneous over length scales of importance to a particular problem. It must be realized that in these cases the model can only be accurate in some average sense at best.

Acknowledgements

This work was sponsored in part by the United States Department of Energy under contract W-7405-ENG-36.

1. W.R.D. Wilson, Strategy for Friction Modeling in Computer Simulations of Metalforming, Proc. NAMRC XVI, SME, 45-84 (1988).

2. N. Bay and T. Wanheim, Real Area of Contact and Friction Stress at High Pressure Sliding Contact,*Wear*,**38**,201-209(1976).

3. W.R.D. Wilson and S. Sheu, Real Area of Contact and Boundary Friction in Metal Forming, *Int. J. Mech. Sci.*, **30**, 475-489 (1988).

4. D.A. Korzekwa, P.R. Dawson and W.R.D. Wilson, Surface Asperity Deformation During Sheet Forming, Submitted to *Int. J. Mech. Sci.*

5. J.A. Greenwood and G.W. Rowe, Deformation of Surface Asperities During Bulk Plastic Flow, *J. Appl. Phys.*,**36**,667-668(1965)

6. A.K. Sengupta, B. Fogg, and S.K. Ghosh, On the Mechanism Behind the Punch-Blank Surface Conformation in Stretch-Forming and Deep-Drawing, *Journal of Mechanical Working Technology,* **5**, 181-210 (1981).

7. A.K. Ghosh, A Method for Determining the Coefficient of Friction in Punch Stretching of Sheet Metals, *Int. J. Mech. Sci.*, **19**, 457-470 (1977).

8. W.R.D. Wilson, "Friction and Lubrication in Sheet Metal Forming", *Mechanics of Sheet Metal Forming*, Proc. Of G. M. Symposium, 1978, Plenum Press, N.Y., pp. 157-177.